

ANALYSIS ON CONSTRUCTION DEFORMATION AND SUPPORTING STRUCTURE OF TWO-STEP AND THREE-SECTION EXCAVATION METHOD FOR SUPER LARGER SPAN HIGHWAY TUNNEL

Fujin Hou¹, Yanbin Luo², Qing Jiang³, Jianxun Chen², Tao Li³, Fangfang Dong²

1. Shandong University, Research Center of Geotechnical and Structural Engineering, No. 27 Shanda South Road, Licheng District, Jinan City, Shandong Province, China; 188978807@qq.com
2. Chang'an University, Highway Institute, Middle Section of Nan Erhuan Road, Xi'an City, Shannxi Province, China; lyb@chd.edu.cn, 563303323@qq.com, chenjx1969@163.com
3. Shandong Expressway Jilai Intercity Highway Co., Ltd. 788 Jingshan Road, Lixia District, Jinan City, Shandong Province, China, 279415652@qq.com, 552126247@qq.com

ABSTRACT

The super larger span tunnel is a common form of highway reconstruction and expansion projects in recent years. In order to determine the stability of tunnel structure of the two-step and three-section excavation method of the III-level surrounding rock mass of the super larger span highway, the field test method was adopted. Relying on the Laohushan Tunnel in Jinan, Shandong, China, the deformation and the structure performance of the super larger span tunnel in III-level surrounding rock mass are analyzed, and the safety of the tunnel and the support structure is evaluated on this basis. The results show that the maximum settlement of the arch section of the Grade III surrounding rock section is 12.5mm, and the maximum clearance convergence is 5.8mm. Both of them are much smaller than the design reserved deformation of 80mm. The maximum pressure of the surrounding rock is 0.091MPa, showing that the force acting on the supporting structure by surrounding rock mass is small. The inner and outer arched parts of the steel frame are subject to large stresses, and most of them are tensile stresses. The maximum stress of the steel frame is 283 MPa, and occurs at the inner side of right arch waist. Although the local stress exceeds the yield strength of the steel (235 MPa), it does not exceed its ultimate compressive strength of 400 MPa, and the tensile and compressive stress values of the other inner and outer parts do not exceed the yield strength. Mainly, the maximum stress appears on the left side wall, reaching 4.83 MPa, which is far less than the ultimate compressive strength of sprayed concrete (11.9 MPa). For super larger span highway tunnels, located in III-level surrounding rock mass, constructed by two-step and three-section excavation method, the initial support effectively controlled the tunnel deformation, the supporting structures were fully protected and the tunnel structure was stable. The super larger span tunnel is a common form in the road reconstruction and expansion project in recent years. In order to determine the stability of tunnel structure of the two steps and three excavation method of the III-level surrounding rock mass of the super larger span highway, the field test method was adopted. Relying on the Laohushan Tunnel, the deformation and the structure performance of the super larger span tunnel in III-level surrounding rock mass were analyzed. The results show that the maximum settlement of arch of the III-level surrounding rock mass is 12.5mm in super larger span highway tunnel, and the maximum clearance convergence is 5.8mm. Both of them are smaller than the design reserved deformation of 80mm. The maximum surrounding rock mass pressure is 0.091MPa, the force acting on the supporting structure by surrounding rock mass are small. The inner and outer arched parts of the

steel frame bear larger stress, and are mostly tensile stress. The maximum stress on inner side of the steel frame is 283 MPa, and occurs at the right arch waist. The maximum stress on the outer side of the steel frame is 184 MPa, and occurs at the vault. The steel frame plays an important role in the initial support, however the force does not reach the yield strength of the steel. The shotcrete is subjected to pressure, the maximum stress appears on the left side wall is 4.83 MPa, which is much smaller than the ultimate compressive strength of shotcrete of 25 MPa. So for super larger span highway tunnels, located in III-level surrounding rock mass, constructed by two-step and three-excitation method, the whole structure is stable.

KEYWORDS

Super larger span highway tunnel, Two-step and three-section excavation method, Deformation, Support structure stress, Analysis

INTRODUCTION

In recent years, with the rapid increase of highway transportation volume, the proportion of super larger span tunnel in the reconstruction and expansion project of highway tunnel are increasing. Many scholars in China have carried out related research on super larger span highway tunnel. For example, combined with actual engineering or numerical model analysis, Qu et al. (2008) and Liu et al (2015) researched the calculation method of surrounding rock mass pressure based on the traditional theoretical calculation method of surrounding rock mass pressure. Taken Guangzhou Longtoushan Tunnel as the engineering background, Zhou et al. (2009a, b; 2011) focused on the deformation rules of surrounding rock mass with time and excavation process of super larger span highway tunnel with the construction of double-side guide pit method. The regularity and the mechanical behaviour of the support system during tunnel construction are also researched. In addition, Yong Zhao, Shucai Li et al (2012) used the Lanyu Railway Liangshui tunnel as the engineering background to research the release process of surrounding rock mass load during tunnel excavation through geomechanical model experiments. According to monitoring and measurement analysis of the Kuiqi 2# tunnel, Jiang et al. (2010) researched the deformation and surrounding rock mass pressure distribution characteristics of the two-way eight-lane small clear distance highway tunnel. The relevant research about super larger span tunnel has achieved certain results at present, but there is no systematic technical specification for the design and construction of super larger span highway tunnel (Zhou et al. 2009b), resulting in the construction method and supporting parameters of super larger span highway tunnel engineering are mixed.

Given that super larger span four-lane highway tunnel structure has flat shape, large span and thin arch wall etc. characteristics, the deformation of surrounding rock mass and mechanical characteristics of support structure are more complicated than the conventional two-lane and three-lane tunnels. Based on the actual engineering, the rules of tunnel deformation, surrounding rock mass deformation and stress of supporting structure of the super larger span highway tunnel was analyzed, under different level of surrounding rock mass conditions with different construction method and supporting parameter. It is the necessary way to confirm reasonable construction method and supporting parameter of super larger span highway tunnel.

Up to now, we only have studies about larger span tunnel and super larger span tunnel with double-wall guide pit method, CRD method and other excavation (e.g. Xia et al. 2007; Gong et al. 2009; Sharifzadeh M. et al. 2013; Li et al. 2014; Zhou et al. 2017), there is almost no research on the construction of two-step three-section excavation method for super larger span tunnel.

METHODS

In this paper, using Laohushan Tunnel, the super larger span highway tunnel as the engineering background, the surrounding rock mass deformation discipline and support structure stress of the super larger span highway tunnel during the construction of the two-step and three-section excavation method of the III-level surrounding rock mass section was researched. Among them, the division of surrounding rock is based on China's *Specifications for Design of Highway Tunnels* (JTG 3370.1-2018).

Engineering survey

Laohushan Tunnel is located in Jinan, Shandong province, China, and is the first two-way eight-lane municipal highway tunnel in Shandong province. The tunnel spans two places, Lixia District and Shizhong District, Jinan. The entrance is located on the southwest side of Huangjin Shanshui County, south of the intersection of Tourism Road and Erhuan East Road, and the exit is located in Bandaoting Village, which is adjacent to the Erhuan Southeast Road as shown in Figure 1.

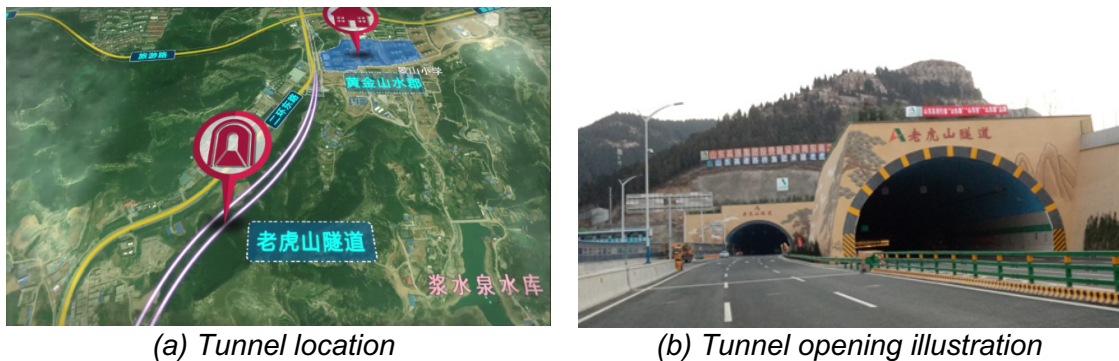


Fig. 1 – Laohushan Tunnel Overview

The maximum excavation span of a single tunnel is 20.08m and the maximum excavation height is 13.4m which belongs to super larger span highway tunnel. The right line of the tunnel is 1888m and the left line is 1740m. Construction started in March 2016 and completed in July 2017. It is the pivotal dominant engineering of the South Extension Project of the Second Ring Road of Jinan Link of Beijing-Shanghai Expressway.

Geological conditions

The fracture structure of the stratum passing through the Laohushan Tunnel is relatively developed, and it has a wide distribution and strong directionality, mainly in the northeast-southwest direction and southeast-northwest direction. The overall area stability is general. The entrance of the tunnel is located at the foot of the mountain. There is a residual layer of slope on the surface layer, and the thickness of the soil layer is about 0.4m to 10.7m. The outcrop layer at the portal of right tunnel entrance is mainly Ordovician limestone, and its strike is perpendicular close to the axis of the cave. The portal of right tunnel is dominated by Yanshanian diorite, joint fissure development.

Support parameters and construction plan

The excavation of the III-level surrounding rock mass section of the Laohushan Tunnel used two-step and three-section excavation method. The construction sequence of the field excavation is shown in Figure 2. (1) Excavation of the upper bench → (2) Excavation of the right side of the lower bench → (3) Excavation on the left side of the lower bench.

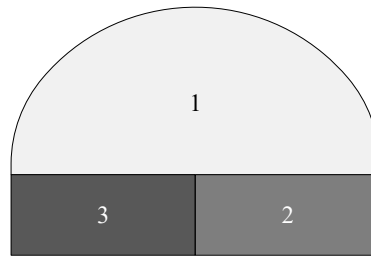


Fig. 2 – Two-step and three-section excavation method

The initial support parameters of the Laohushan Tunnel are shown in Figure 3. The steel frame is made of I18 I-beam, with a longitudinal distance of 120 cm. The steel frame was welded with 20 cm × 20 cm steel mesh and $\Phi 22$ mm anchor rod was placed at the vault, 30°, 60°, and arched which length $L=350$ cm.

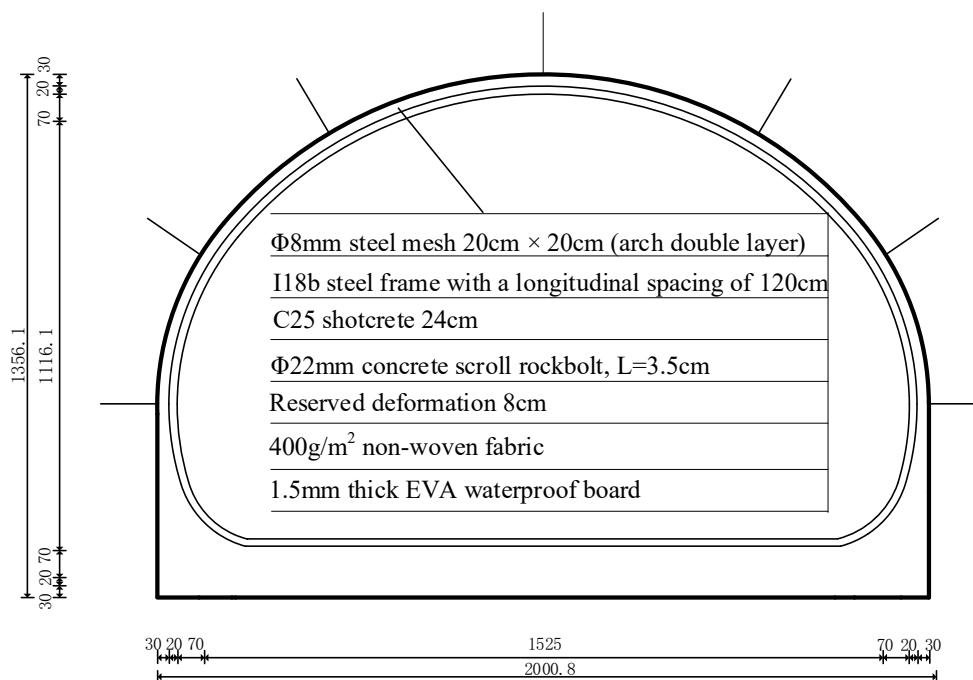


Fig. 3 – Initial support parameters of the Laohushan Tunnel

Monitoring measurement plan

Selection of monitoring and measuring section about III-level surrounding rock mass

The monitoring section of the two-step construction of the Laohushan Tunnel was selected on the right line, and the mileage of the section is YK2+860. The section is far away from the rescue passage of the Laohushan Tunnel, and serves as construction guide hole during the construction period. Avoiding the interference of factors such as the increase of the span at the intersection of the construction guide hole and the main hole. Meanwhile, the construction of the III-level surrounding rock mass section of the left tunnel was postponed to two months after the YK2+860 section is monitored. So the monitoring and measurement of the III-level surrounding rock mass section excavated by two-step and three-section excavation method of right-hole tunnel is carried out, which can provide a reliable reference for the construction of the III-level surrounding rock mass of the left hole later. The surrounding rock condition of III-level surrounding rock section in the tunnel is shown in Figure 4.



Fig. 4 – Monitoring section rock condition

Monitoring measurement point arrangement

According to the requirements of China's "Technical Specifications for Highway Tunnel Construction" (JTJ F60-2009), combined with the structural characteristics and construction methods of the Laohushan super larger span tunnel, the monitoring and measurement projects were developed, which includes deformation monitoring and force monitoring. Among them, the deformation monitoring has arch settlement and clear air convergence, the force monitoring includes surrounding rock mass pressure, shotcrete stress, steel frame stress, etc. And the key parts of tunnel construction are tracked and monitored. In view of the two-step and three-section excavation method used in the tunnel monitoring and measuring section, and the excavation of the right side of the lower bench is delayed for 50 days, which is compared with the upper bench. There is no condition for the deformation monitoring point at the lower bench. The deformation monitoring measurement scheme is determined to arrange five settlement deformation monitoring points and 2'-3', 4'-5' horizontal convergence deformation lines around the arch of upper bench, as shown in Figure 5 The layout of stress monitoring components including surrounding rock mass pressure, steel frame stress, and concrete stress is shown in Figure 4 With the initial support of tunnel face, the stress monitoring components of the corresponding parts of 0~6 in Figure 6 are buried, and the corresponding 7 and 8 parts of Figure 6 are buried respectively after the subsequent step excavation.

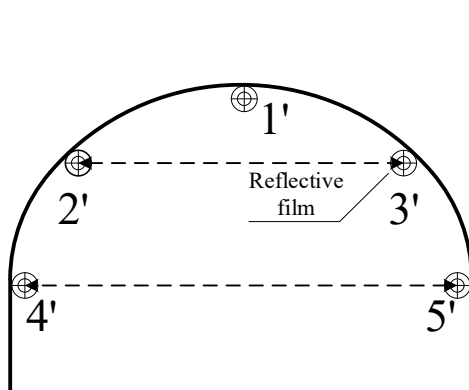


Fig. 5 – Monitoring point layout

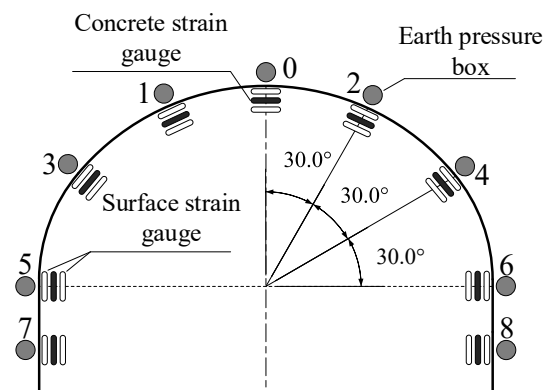


Fig. 6 – Stress monitoring component layout

RESULTS

Deformation monitoring results analysis

Arch settlement

The on-site monitoring and measurement data of YK2+860 section arch settlement is shown in Table 1. The arch settlement curve is shown in Figure 7.

Tab. 1 - Monitoring results of arch settlement in monitoring section

Position	Test section	Maximum settlement value/mm	Cumulative settlement/mm
Vault (1')	YK2+860	8.6	7.2
Left arch waist (2')	YK2+860	2.4	2.3
Right arch waist (3')	YK2+860	4.8	4.5
Left arch (4')	YK2+860	3.2	2.8
Right arch (5')	YK2+860	12.5	10.9

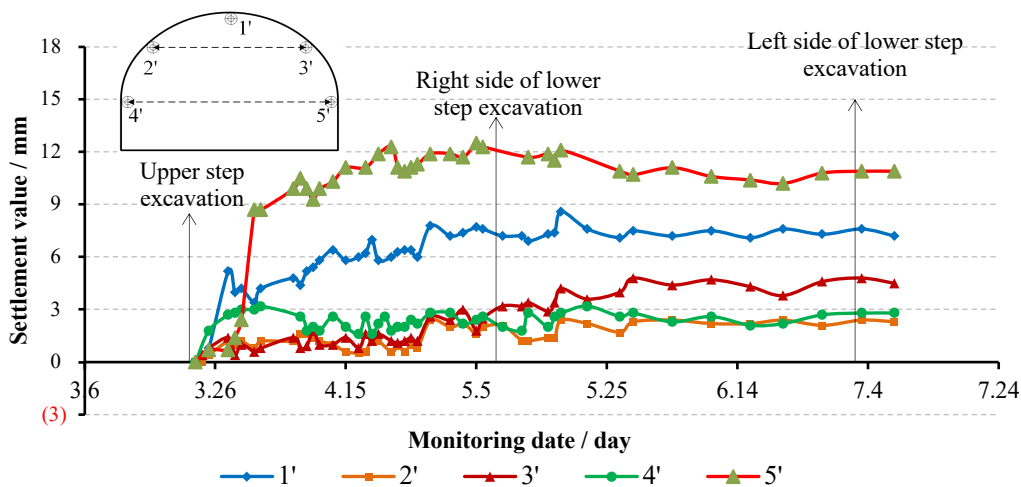


Fig. 7 –Settlement temporal curve on YK2+860 section

It can be seen from Table 1 that the maximum settlement value of the vault of the YK2+860 section is 8.6 mm. The maximum settlement value of the left arch waist is 2.4 mm, the maximum settlement value of the right arch waist is 4.8 mm, and the maximum settlement value of the left wall is 3.2mm, the maximum settlement value of the right wall is 12.5mm. It can be seen that the settlement deformation of the monitoring section in the initial support stage is relatively small.

It can be seen from the sedimentation temporal curve in Figure 7 that the settlement values of 1' point (vault) and 5' point (right wall) are relatively large, and the settlement values after stabilization are about 11mm and 8mm, respectively. The settlement amplitudes of the monitoring points are not much different, and are less than 5 mm. After the excavation of the tunnel face, the sedimentary temporal curve of each monitoring point generally appears as three stages: rapid growth, slow growth and steadiness. Rapid growth stage: the settlement value increases rapidly in the week after the step excavation on the monitoring section. The cumulative settlement at this stage accounts for about 75% of the total settlement. The slow growth stage, 2~5 weeks after the step excavation on the monitoring section, the sedimentation temporal curve slowly rises. Due to

the influence of the excavation of the front face, the settlement curve has a small fluctuation, but the overall trend keeps growing slowly. The stationary phase: the step excavation on the monitoring section is 5 weeks. After that, the subsidence enters the stable phase from the slow growth phase and gradually stabilizes. Affected by factors such as blasting vibration during construction, the sedimentation time curve has slight fluctuations, but the overall stability is stable. The settlement values of each point after stabilization are different, but they are all within 13mm, which is much smaller than the designed deformation of 80mm.

Clearance convergence

The field monitoring and measurement data of YK2+860 section surrounding rock mass convergence are listed in Table 2, and the headroom convergence time curve is shown in Figure 8.

Tab. 2 - Monitoring section convergence deformation monitoring results

Position	Monitoring section	Maximum convergence value / mm	Cumulative convergence value / mm
Arch waist convergence (2-3)	YK2+860	2.8	2.4
Arch foot convergence (4-5)	YK2+860	5.8	3.8

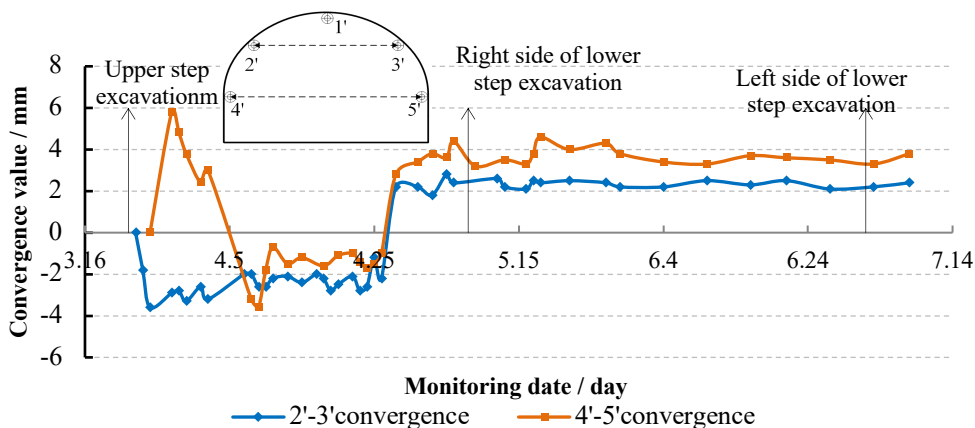


Fig. 8 –Convergence temporal graph on YK2+860 section

It can be seen from Table 2 that the maximum convergence value of the 2'-3' at the waist of the YK2+860 section is 2.8mm, and the maximum convergence value of the 4'-5' at the arch is 5.8mm, and the cumulative convergence values at the arch waist and the arch foot are respectively 2.4mm and 3.8mm.

From Figure 8 of the YK2+860 cross-section headroom convergence, it can be seen that after the excavation of the tunnel face, the convergence around the tunnel shows a negative value, indicating that the initial support and surrounding rock mass occur a certain expansion deformation under the load of the upper part of the surrounding rock mass. The expansion deformation of the arch waist in the horizontal direction is between 2.0 and 3.5 mm, and the expansion deformation of the arch is slightly smaller than that of the arch waist, which is between 0.5 and 2.0 mm. Under the influence of excavation, redistributed surrounding rock mass pressure and so on, the convergence deformation temporal curve has obvious fluctuations at this stage, but the deformation value is small overall. As the tunnelling surface on the right side of the lower bench gradually approaching the monitoring section, due to the influence of its construction disturbance, the headroom convergence occurs in the horizontal direction, and the convergence value suddenly increases

above the abscissa, and the convergence value of the arch waist fluctuates slightly above and below 2.0 mm. The convergence of the arch foot is larger than that of the arch waist, and the convergence value fluctuates slightly above and below 4.0 mm. After the right side of the lower bench has been dug into the monitoring section, the convergence deformation time curve of the arch waist and the arch foot tend to be stable, and the tunnelling construction of the lower bench's left side which is near the monitoring section has no obvious influence on the convergence deformation.

It can be seen that the super larger span highway tunnel is constructed by two-step and three-section excavation method in the class III surrounding rock mass. The maximum settlement of the arch is 12.5mm. The maximum convergence of the clearance is 5.8mm, and the deformation is much smaller than the designed deformation which is 80mm.

Analysis of stress monitoring results

Surrounding rock mass pressure

Monitoring is from March 22, 2017, when the components were buried, to July 18, 2017, when the secondary lining was applied. The maximum surrounding rock mass pressure during this period is listed in Table 3. The variation curve of surrounding rock mass pressure is shown in Figure 7. The numbers in Table 3 and Figure 7 indicate different parts, and the specific parts are shown in the cross section of Figure 9.

Tab. 3 - Distribution of pressure values of surrounding rock mass on YK2+860 section

Measuring point	Maximum pressure value / MPa	Measuring point	Maximum pressure value / MPa
Y0	0.009	Y5	0.009
Y1	0.018	Y6	0.012
Y2	0.052	Y7	0.013
Y3	0.091	Y8	0.007
Y4	0.019		

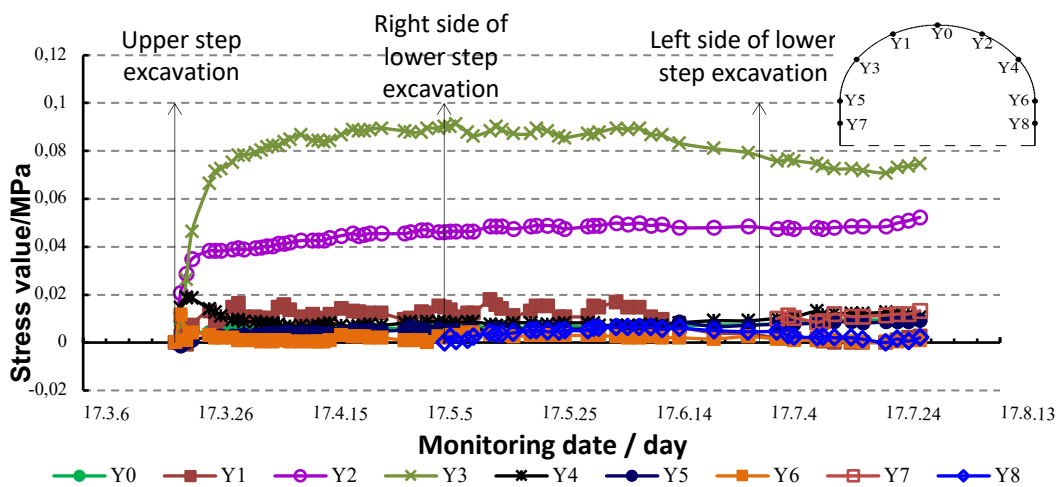


Fig. 9 –Temporal curve of surrounding rock pressure on YK2+860 section

It can be seen from Table 3 that the maximum value of the surrounding rock mass pressure of the YK2+860 section appears at the left arch waist (Y3), the value is 0.091 MPa. And the value of the surrounding rock mass pressure at 30° to the right of vault (Y2), which comes second, is 0.052 MPa. The rest of the surrounding rock mass pressure is relatively small, all less than 0.020MPa, indicating that the surrounding rock mass acts less on the supporting structure.

From the surrounding rock mass pressure temporal curve in Figure 9, it can be seen that except for the right arch waist 30 ° (Y2) and the left arch waist (Y3), the surrounding rock mass pressures of all other points are within 0.020 MPa. The pressure of the surrounding rock mass at the right arch waist 30° (Y2) and the left arch waist (Y3) is relatively large, and it is about 0.05MPa and 0.08MPa respectively after stabilization and the surrounding rock mass exerts less force on the support. The variation trend of the surrounding rock mass pressure temporal curve is similar. The curve increases sharply within 7 days after the excavation of the upper bench, and then quickly stabilizes. The overall trend of the stabilized tense curve is stable and the change is slow. The lower bench excavation process has no significant effect on the surrounding rock mass pressure at upper bench arch.

Steel frame stress

The maximum stress of YK2+860 section steel frame at the initial monitoring points are listed in Table 4 and Table 5. The stress temporal curves of the monitoring section steel frame at inner and outer sides are shown in Figure 10 and Figure 11. In Figure 10 and Figure 11, the letter "B" in B0-1 indicates the steel frame stress, and the numbers indicate different "parts - inner and outer sides" (the outer side indicates the side which the flange plate of steel frame is near the surrounding rock mass "-1", the inner side indicates the side which the flange plate of steel frame is away from the surrounding rock mass "-2"). The positive value indicates that the steel frame stress is compressive stress while the negative value indicates that the steel frame stress is tensile stress.

Tab. 4 - Stress distribution on the outer side of steel frame on YK2+860 section

Measuring point	Maximum stress value / MPa	Measuring point	Maximum stress value / MPa
B0	165	B5	55
B1	120	B6	-48
B2	113	B7	22
B3	-	B8	-24
B4	184		

Tab. 5 - Stress distribution on the inner side of steel frame on YK2+860 section

Measuring point	Maximum stress value / MPa	Measuring point	Maximum stress value / MPa
B0	103	B5	-55
B1	81	B6	-35
B2	283	B7	-11
B3	-2	B8	23
B4	56		

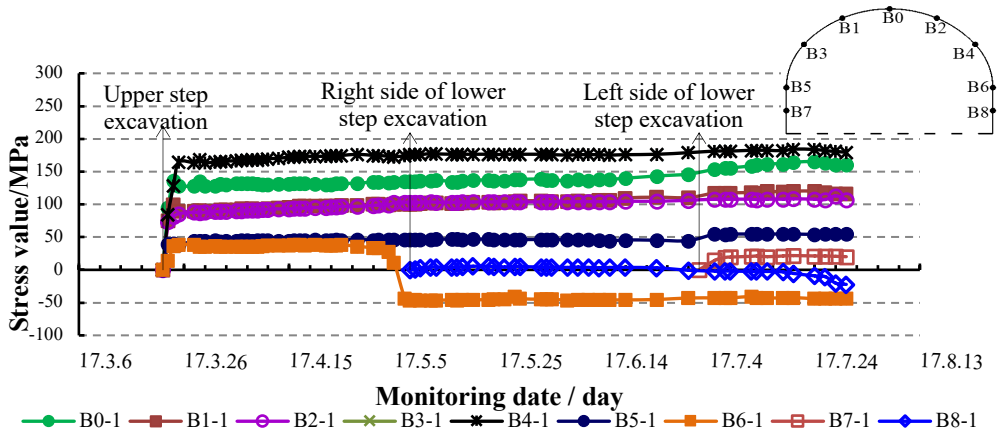


Fig. 10 – Temporal curve of stress on the outer side of steel frame on YK2+860 section

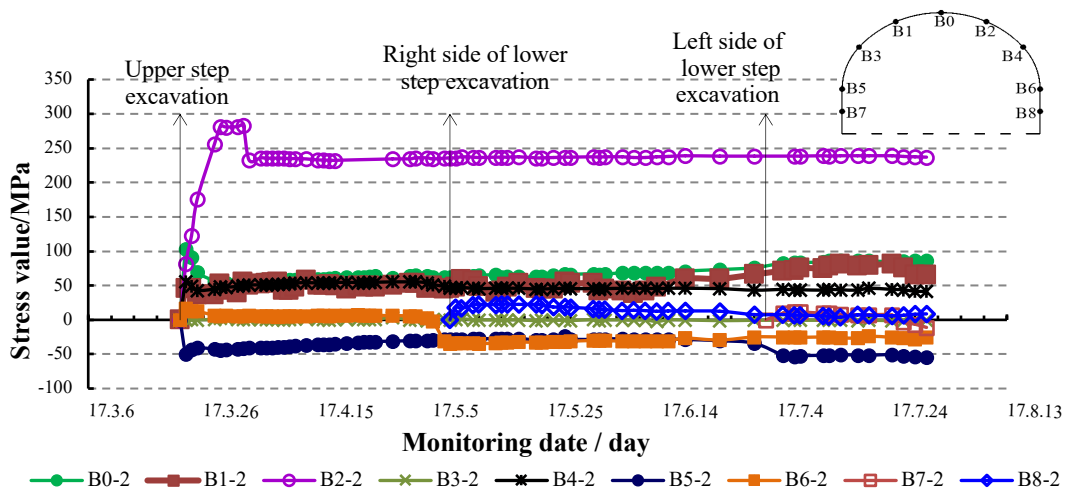


Fig. 11 – Temporal curve of stress on the inner side of steel frame on YK2+860 section

According to Table 4 and Table 5, the stress on the steel frame changes greatly and the load distribution is uneven. From the overall structure, the inner and outer arches (B0, B1, B2, B4) of the steel frame are subjected to large forces, and the compressive stress is the main one. The force at the side wall is small, and the tensile stress is mostly. The steel frame stress, especially the outer edge of the arch, is mainly composed of compressive stress, which indicates that the steel frame effectively played the role of bearing and restricting the deformation of the surrounding rock mass. The maximum stress on the outer side of the steel frame occurs at the arch waist, the value is 184 MPa, and the maximum stress on the inner side of the steel frame occurs at 30° of the right arch waist, the value is 283 MPa, which indicates that the steel frame is subjected to large force and plays the role of bearing and restricting the surrounding rock mass deformation.

From the stress temporal curves of the inner and outer side of the steel frame in Figure 10~11, it can be seen that the stress increases sharply within 1~7 days after the steel frame is applied; the steel frame tends to be stable after 7 days of application, and the stress value of the steel frame changes little with time at this stage. Due to the excavation construction on the right side of the lower bench, the state of the steel frame stress at the right arch (B6) is abrupt. The internal and external compressive stresses of B6 steel frame before May 4, 2017 were 2 MPa and 34 MPa respectively. After the excavated section on the right side of the lower bench approached and exceeded the monitoring section within four days from May 5 to 8, 2017, the internal steel frame stress suddenly changed to tensile stress, and the internal and external tensile stress values

were 35 MPa and 46 MPa, respectively. The time for the abrupt deformation to mutate is more consistent.

Shotcrete stress

The maximum concrete stress of YK2+860 section is shown in Table 6. The stress temporal curve of shotcrete is shown in Figure 10. The parts corresponding to the numbers in Table 7 and Figure 10 are shown in the schematic diagram of the components' position in Figure 12. The positive values in Table 6 and Figure 12 are the compressive stress and the negative value is the tensile stress.

Tab. 6 - Stress distribution of shotcrete on YK2+860 section

Measuring point	Maximum stress value / MPa	Measuring point	Maximum stress value / MPa
0	0.81	5	4.83
1	2.51	6	2.58
2	3.99	7	-0.84
3	1.89	8	-0.71
4	3.80		

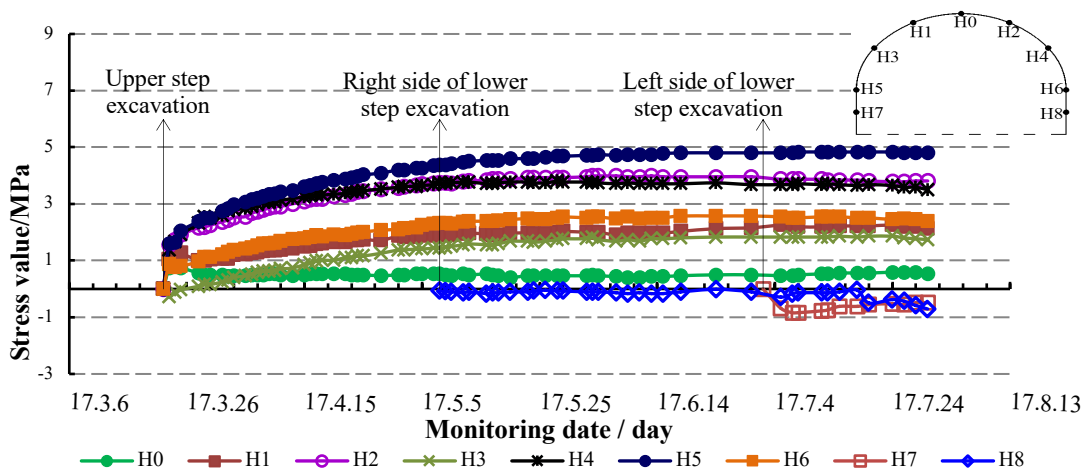


Fig. 12 – Stress temporal curve of shotcrete on YK2+860 section

It can be seen from Table 6 that the concrete of the test section is mainly pressed. The maximum compressive stress of concrete at the monitoring section appears at the left side wall, and its value is 4.83 MPa. The maximum concrete stress is much smaller than 25 MPa, which is the ultimate compressive strength of shotcrete.

It can be seen from Figure 12 that the development trend of the shot concrete stress temporal curve of each monitoring point is basically the same for YK2+860 section. The stress growth is faster within 7 days after the application of the shotcrete, and the stress growth is slow after 7 days of application. After 60 days of application, the stress value is basically in a stable state, and the step construction process has no obvious influence on the concrete stress state.

To sum up, it can be seen that for super larger span highway tunnels constructed using two-step and three-section excavation method for III-level surrounding rock mass, the deformation and the force of support structure are relatively small after the excavation of the upper bench. The supporting structure can well restrain the deformation of the surrounding rock mass and make the surrounding rock mass enter the stable state in a short time. The subsequent lower bench construction will have less influence on the deformation of the tunnel and the support structure.

Safety evaluation of tunnels and supporting structures

According to the monitoring results of the tunnel deformation and supporting structure stress of YK2 + 860 section, the safety of each supporting structure was evaluated. The detailed evaluation contents are listed in Table 7.

Tab. 7 - Safety evaluation of tunnel and supporting structures on YK2 + 860 section

Monitoring project		Position	Maximum value	Design value	Proportion (maximum / design)	
Initial support	Arch settlement (mm)	Right arch foot (5')	12.5	80	16%	
	Clearance convergence (mm)	Arch foot (4-5)	5.8	80	7%	
Surrounding rock pressure		Left arch waist 60° (3)	0.091	/	/	
Shotcrete stress (MPa)	Compressive stress	Left arch foot (5)	4.83	11.9	41%	
	Tensile stress	Left wall foot (7)	-0.84	-1.27	66%	
Steel frame stress (MPa)	Outside	Compressive stress	Right arch waist 60° (4)	184	235	78%
		Tensile stress	Right arch foot (6)	-48	-235	20%
	Inside	Compressive stress	Right arch waist 30° (2)	283	235	120%
		Tensile stress	Left arch foot (5)	-55	-235	23%

It can be known from Table 7 that the maximum value of the initial settlement of the supporting arch in this section is 12.5mm, and the maximum value of headroom convergence is 5.8mm, which is far less than the designed deformation of 80mm. The maximum value of surrounding rock pressure appeared at 60° of the left arch waist, reaching 0.091 MPa. The local compressive stress on the inner side of the steel frame exceeds the yield strength of the steel 235 MPa, but it does not exceed the ultimate compressive strength of the steel 400 MPa, and the tensile and compressive stress values of the other inner and outer parts do not exceed the yield strength (up to 78% of the yield strength). The maximum compressive and tensile stresses of shotcrete are located at the left arch foot and wall foot respectively, and they do not exceed the design tensile and compressive strength of C25 shotcrete.

CONCLUSION

Based on the above monitoring measurement data analysis, the following conclusions can be drawn:

- (1) For super larger span highway tunnels, located in III -level surrounding rock mass, constructed by two-step and three-section excavation method, the maximum arch settlement is 12.5 mm, the maximum clearance is 5.8 mm, and the deformation is much smaller than the designed deformation of 80mm. After digging, the effect of support to control tunnel deformation is better.
- (2) For super larger span highway tunnels, located in III-level surrounding rock mass, constructed by two-step and three-section excavation method, the maximum value of surrounding rock pressure is 0.091 MPa. According to engineering experience, this value is within the normal

range of class III surrounding rock pressure and acts on the support. The force on the protective structure is small.

(3) For super larger span highway tunnels, located in III-level surrounding rock mass, constructed by two-step and three-section excavation method, the inner and outer arches of the steel frame are subject to large stresses and mostly tensile stresses, although the local compressive stress on the inside of the steel frame exceeds the yield strength of the steel 235 MPa but did not exceed the ultimate compressive strength of the steel 400 MPa, and the tensile and compressive stress values of the other inner and outer parts did not exceed the yield strength (up to only 78% of the yield strength), indicating that the steel frame played an important role in the initial support. The shotcrete is mainly compressed, and its maximum compressive and tensile stresses are located at the left arch foot and the wall foot respectively, and both do not exceed the design tensile and compressive strength of the C25 shotcrete.

(4) Based on the comprehensive test results of tunnel deformation and supporting structure stress, it can be seen that after the two-stage and three-section excavation method of the III-stage surrounding rock section of a super-long-span highway tunnel, the initial support effectively controlled the tunnel deformation, and each stress of supporting structures was safety, the tunnel structure is stable.

ACKNOWLEDGEMENTS

The authors would like to acknowledge the financial support provided by the national key research and development program (grant no. 2016yfc0802202), the national natural science fund project of china (grant nos.51108034, 51408054 and 51678063), the china postdoctoral science foundation (grant no.2016m602738), the basic research project of natural science in shaanxi province (grant no. 2017jm5051) and the chang jiang scholars program (grant no. T2014214).

REFERENCES

- [1] Barton N, Lien R, Lunde J, 1974. Engineering classification of rock masses for the design of tunnel support Publikasjon - Norges Geotekniske Institutt
- [2] Bizjak KF, Petkovek B, 2004. Displacement analysis of tunnel support in soft rock around a shallow highway tunnel at Golovec Engineering Geology 75:89-106 doi:10.1016/j.enggeo.2004.05.003
- [3] Chen J-J, Zhou F, Yang J-S, Liu B-C, 2009. Fuzzy analytic hierarchy process for risk evaluation of collapse during construction of mountain tunnel Yantu Lixue/Rock and Soil Mechanics 30:2365-2370
- [4] Choi SO, Chung S-K, 2004. Stability analysis of jointed rock slopes with the barton-bandis constitutive model in udec International Journal of Rock Mechanics and Mining Sciences 41:2B 20 21-26 doi:10.1016/j.ijrmms.2004.03.103
- [5] Fang Q, Su W, Zhang D, Yu F, 2016. Tunnel deformation characteristics based on on-site monitoring data Yanshilixue Yu Gongcheng Xuebao/Chinese Journal of Rock Mechanics and Engineering 35:1884-1897 doi:10.13722/j.cnki.jrme.2014.1663
- [6] Gong J-W, Xia C-C, Zhu H-H, Tang Y, 2009. Optimal analysis of construction schemes for Heshang small-space tunnels with large section Yantu Lixue/Rock and Soil Mechanics 30:236-240
- [7] Gonzalez-Nicieza C, Alvarez-Vigil AE, Menendez-Diaz A, Gonzalez-Palacio C, 2008. Influence of the depth and shape of a tunnel in the application of the convergence-confinement method Tunnelling and Underground Space Technology 23:25-37 doi:10.1016/j.tust.2006.12.001
- [8] Jiang K, Xia C, 2010. Analysis of monitoring and measurement of small clear spacing highway tunnel with eight lanes Yanshilixue Yu Gongcheng Xuebao/Chinese Journal of Rock Mechanics and Engineering 29:3755-3761
- [9] Jiang Y, Yoneda H, Tanabashi Y, 2001. Theoretical estimation of loosening pressure on tunnels in soft rocks Tunnelling and Underground Space Technology 16:99-105 doi:10.1016/S0886-7798(01)00034-7

- [10] Li P, Zhao Y, Zhang D, Wu D, 2013. Study of distribution laws of tunnel surrounding rock pressure based on field measured data statistics *Yanshilixue Yu Gongcheng Xuebao/Chinese Journal of Rock Mechanics and Engineering* 32:1392-1399
- [11] Li S, Yuan C, Feng X, Li S, 2016. Mechanical behaviour of a large-span double-arch tunnel *KSCE Journal of Civil Engineering* 20:2737-2745 doi:10.1007/s12205-016-0456-y
- [12] Liu Y-P, He S-H, Wang D-H, Li D-Y, 2015. Study of surrounding rock pressure calculation of deep super-span underground structures *Yantu Lixue/Rock and Soil Mechanics* 36:118-124 doi:10.16285/j.rsm.2015.S2.015
- [13] Priest SD, 2005. Determination of shear strength and three-dimensional yield strength for the Hoek-Brown criterion *Rock Mechanics and Rock Engineering* 38:299-327 doi:10.1007/s00603-005-0056-5
- [14] Qu H-F, Zhu H-H, Cai Y-C, 2008. Discussion on calculation of loose load on extra-large cross-section and large-span road tunnel *Yantu Lixue/Rock and Soil Mechanics* 29:989-994+1000
- [15] Sharifzadeh M, Kolivand F, Ghorbani M, Yasrobi S, 2013. Design of sequential excavation method for large span urban tunnels in soft ground - Niayesh tunnel *Tunnelling and Underground Space Technology* 35:178-188 doi:10.1016/j.tust.2013.01.002
- [16] Shen B, Barton N, 1997. The disturbed zone around tunnels in jointed rock masses *International journal of rock mechanics and mining sciences & geomechanics abstracts* 34:117-125 doi:10.1016/S0148-9062(96)00048-4
- [17] Singh B, Goel RK, Jethwa JL, Dube AK, 1997. Support pressure assessment in arched underground openings through poor rock masses *Engineering Geology* 48:59-81 doi:10.1016/S0013-7952(97)81914-X
- [18] Wu Q-J, Wang M-N, Liu D-G, 2012. Research on stability of tunnel surrounding rocks based on statistical analysis of on-site displacement monitoring data *Yantu Lixue/Rock and Soil Mechanics* 33:359-364
- [19] Xia C, Gong J, Tang Y, Zhu H, 2007. Study on site monitoring of large-section highway tunnels with small clear spacing *Yanshilixue Yu Gongcheng Xuebao/Chinese Journal of Rock Mechanics and Engineering* 26:44-50
- [20] Zeng S, Qin Q-T, Yang J-S, 2008. In-situ monitoring behaviors of middle wall of large-span multi-arch tunnel *Yantu Lixue/Rock and Soil Mechanics* 29:2537-2541
- [21] Zhang G-H, Chen L-B, Qian S-X, Cai G-Y, Wu C-F, Li Q, 2010. On-site supervision measure and analysis of Damaoshan tunnels with large section and small clear-distance *Yantu Lixue/Rock and Soil Mechanics* 31:489-496
- [22] Zhou D, Cao L, Ma Y, Fang S Stability monitoring and analysis of core rock in a tunnel with extra-large cross section and low flat-ratio during construction. In: 2011 GeoHunan International Conference - Tunnel Management, Emerging Technologies, and Innovation, June 9, 2011 - June 11, 2011, Hunan, China, 2011. Geotechnical Special Publication. American Society of Civil Engineers (ASCE), pp 56-63. doi:10.1061/47632(411)8
- [23] Zhou D, Cao L, Qu H, Yi L, Fang S, 2009. Deformation monitoring and control of super large section highway tunnel with different surrounding rocks *Yanshilixue Yu Gongcheng Xuebao/Chinese Journal of Rock Mechanics and Engineering* 28:2510-2519
- [24] Zhou D, Qu H, Cai Y, Cao L, Yang H, 2009. In-situ test on surrounding rock deformation in super-large section and large-span tunnel *Yanshilixue Yu Gongcheng Xuebao/Chinese Journal of Rock Mechanics and Engineering* 28:1773-1782
- [25] Zhou Z, Li J, Jin B, Liu Y Numerical Investigation of the Optimal Construction Sequence of an Actual Super Shallow Large-Span Tunnel. In: World Multidisciplinary Civil Engineering-Architecture-Urban Planning Symposium 2017, WMCAUS 2017, June 12, 2017 - June 16, 2017, Prague, Czech republic, 2017. IOP Conference Series: Materials Science and Engineering. Institute of Physics Publishing. doi:10.1088/1757-899X/245/2/022003